

- comparable conditions—i.e., the same metal, molecule or molecules, and temperature—so as to have a more precise and incisive test of the analogy.
- (11) E. L. Muetterties, T. N. Rhodin, E. Band, C. Brucker, and W. R. Pretzer, *Chem. Rev.*, to be published.
  - (12) V. W. Day, R. O. Day, J. S. Kristoff, F. J. Hirsekorn, and E. L. Muetterties, *J. Am. Chem. Soc.*, **97**, 2571 (1975).
  - (13) M. G. Thomas, E. L. Muetterties, R. O. Day, and V. W. Day, *J. Am. Chem. Soc.*, **98**, 4645 (1976).
  - (14) V. W. Day, S. S. Abdell-Meguid, S. Dabestini, M. G. Thomas, W. R. Pretzer, and E. L. Muetterties, *J. Am. Chem. Soc.*, **98**, 8289 (1976).
  - (15) E. Band, W. R. Pretzer, M. G. Thomas, and E. L. Muetterties, *J. Am. Chem. Soc.*, **99**, 7380 (1977).
  - (16) E. L. Muetterties, *Bull. Soc. Chim. Belg.*, **85**, 451 (1976).
  - (17) G. A. Somorjai, *Catal. Rev.*, **7**, 87 (1972).
  - (18) E. L. Muetterties, *Angew. Chem., Int. Ed. Engl.*, **17**, 545 (1978).
  - (19) E. L. Muetterties, J. C. Hemminger, and G. A. Somorjai, *Inorg. Chem.*, **16**, 3381 (1977).
  - (20) Bonding of type **2** is established only for  $\text{CF}_3\text{CN}$  in a platinum complex<sup>21</sup> and for a cyanamide,  $\text{C}_5\text{H}_{10}\text{NCN}$ , in a nickel complex.<sup>22</sup> B. N. Stornoff and A. C. Lewis, Jr., *Coord. Chem. Rev.*, **23**, 1 (1977).
  - (21) W. J. Bland, R. D. W. Kenmitt, and R. D. Moore, *J. Chem. Soc., Dalton Trans.*, 1292 (1973).
  - (22) K. Krogmann and R. Maffes, *Angew. Chem., Int. Ed. Engl.*, **5**, 1046 (1966).
  - (23) E. L. Muetterties, *Bull. Soc. Chim. Belg.*, **85**, 45 (1976).
  - (24) See the discussion in E. L. Muetterties, W. R. Pretzer, M. G. Thomas, B. F. Beier, D. L. Thorn, V. W. Day, and A. B. Anderson, *J. Am. Chem. Soc.*, **100**, 2090 (1978).
  - (25) V. W. Day, R. O. Day, J. S. Kristoff, F. J. Hirsekorn, and E. L. Muetterties, *J. Am. Chem. Soc.*, **97**, 2571 (1975).
  - (26) In coordination and cluster chemistry, an acetonitrile ligand is a good leaving group; it is readily displaced by a variety of ligands, including carbon monoxide. With a binding mode as in **3** or **4**, facile acetonitrile desorption or displacement would not be expected. In an analogous case the dihapto binding of an acetylene to a single metal atom is not especially robust. The bond energy, in coordination compounds, is closely similar for those of dihapto olefin-metal and carbon monoxide-metal bonds. However, the binding of acetylenes in a fashion analogous to **3** and **4** is quite strong as judged by chemical studies.<sup>24</sup>
  - (27) G. W. Parshall, *Acc. Chem. Res.*, **3**, 139 (1970); **8**, 113 (1975).
  - (28) D. E. Webster, *Adv. Organomet. Chem.*, **15**, 147 (1977).
  - (29) B. J. Argento, P. Fitton, J. E. McKeon, and E. A. Ruk, *Chem. Commun.*, 1427 (1969).
  - (30) In nickel group metal cyanides, there is a linear  $\text{M}-\text{C}\equiv\text{N}-\text{M}$  array with an overall net-like geometry that is impossible for the nickel(111) surface. A. F. Wells, "Structural Inorganic Chemistry", 4th ed., Clarendon Press, Oxford, 1975, p 967.
  - (31) (a) The cyanogen structures on nickel(111) are now being examined through photoemission studies by Professor D. A. Shirley and his co-workers. (b) E. L. Muetterties and H. Choi, to be published. A problem in this study is the preparation of pure  $\text{Ni}(\text{CN})_2$ .
  - (32) (a) F. T. Netzer, *Surf. Sci.*, **61**, 343 (1976); (b) R. A. Wille, F. T. Netzer, and J. A. D. Matthew, *ibid.*, **68**, 259 (1977); (c) H. Conrad, J. Koppers, F. Nitschke, and F. T. Netzer, *ibid.*, **46**, 571 (1977); (d) M. E. Bridge and R. M. Lambert, *ibid.*, **63**, 315 (1977).
  - (33) M. J. S. Dewar, *Bull. Soc. Chim. Fr.*, **18**, C71 (1951).
  - (34) J. Chatt and L. H. Duncanson, *J. Chem. Soc.*, 2939 (1953).
  - (35) (a) L. L. Kesmodel, R. C. Baetzold, and G. A. Somorjai, *Surg. Sci.*, **66**, 299 (1977); (b) P. C. Stair and G. A. Somorjai, *J. Chem. Phys.*, **66**, 2036 (1977).
  - (36) J. E. Demuth, *Surf. Sci.*, **69**, 365 (1977).
  - (37) H. Ibach, H. Hopster, and B. Sexton, *Appl. Surf. Sci.*, **1**, 1 (1977).
  - (38) L. L. Kesmodel, L. H. Dubois, and G. A. Somorjai, *Chem. Phys. Lett.*, **56**, 267 (1978).
  - (39) (a) A. J. Deeming, S. Hasso, M. Underhill, A. J. Canty, B. F. G. Johnson, W. Jackson, J. Lewis, and T. W. Matheson, *J. Chem. Soc., Chem. Commun.*, 807 (1974); (b) A. J. Deeming and M. Underhill, *J. Organomet. Chem.*, **42**, C60 (1972).
  - (40) H. Conrad, G. Ertl, J. Koppers, and E. E. Latta, *Surf. Sci.*, **57**, 475 (1976).
  - (41) J. E. Demuth, *Surf. Sci.*, **65**, 369 (1977).

## Structure of the Iron-Containing Core in Ferritin by the Extended X-ray Absorption Fine Structure Technique

S. M. Heald,<sup>1a</sup> E. A. Stern,<sup>\*1a</sup> B. Bunker,<sup>1a</sup> E. M. Holt,<sup>1b</sup> and S. L. Holt<sup>1b</sup>

Contribution from the Physics Department, University of Washington, Seattle, Washington 98195, and the Department of Chemistry, University of Wyoming, Laramie, Wyoming 82071. Received April 26, 1978

**Abstract:** Extended X-ray absorption fine structure (EXAFS) measurements are used to determine the structure of the iron-containing core of ferritin. By comparing the EXAFS from ferritin with that from an Fe-glycine model compound, it is found that at room temperature the irons are surrounded by  $6.4 \pm 0.6$  oxygens at  $1.95 \pm 0.02 \text{ \AA}$  which are likely in a distorted octahedral arrangement. Each iron also has  $7 \pm 1$  iron neighbors at an average distance of  $3.29 \pm 0.05 \text{ \AA}$ . Considerable structural disorder was found which increased when the ferritin solution was frozen, indicating a possible phase transition occurring at lower temperatures. Combining these results with the known stoichiometry and density it is shown that the structure for the iron core is a layered arrangement with the iron in the interstices between two nearly close-packed layers of oxygens with approximate sixfold rotational symmetry, and that these compact O-Fe-O layers are only weakly bound to adjacent layers. The known phosphorus component is accounted for by terminating the layer into a strip whose width naturally explains the size of the core. The ferritin core consists, in this picture, of a strip folded back and forth upon itself in the form of a pleat. Measurements are also presented for two forms of the polymer of Spiro and Saltman, and it is found that only one form is possibly similar to ferritin.

### I. Introduction

Iron is stored in animal tissue in two forms, ferritin and haemosiderin. Of the two, the nature and role of ferritin are the better understood.<sup>2</sup> Ferritin is a water-soluble protein which consists of an inorganic  $(\text{FeOOH})_8(\text{FeO}\cdot\text{OPO}_3\text{H}_2)$  micellar core<sup>3,4</sup> approximately  $70 \text{ \AA}$  in diameter surrounded by an organic "shell", with a total diameter of  $\sim 120 \text{ \AA}$ .<sup>5,6</sup> When the protein is "full" of iron it has a molecular weight of approximately 900 000 which is nearly equally divided between the outer sheath and the micellar core. The iron in the core is known to be trivalent.<sup>7</sup>

Magnetic susceptibility and Mössbauer spectroscopic measurements<sup>7,8</sup> have shown conclusively that the  $\text{Fe}^{3+}$  ions

in ferritin are exchange coupled, giving rise to superparamagnetic behavior. This, along with the stoichiometry, has led to the postulation that the  $\text{Fe}^{3+}$  ions in ferritin are connected by  $\text{O}^{2-}$  and  $\text{OH}^-$  bridges.<sup>9,10</sup>

Based upon X-ray diffraction patterns of horse spleen haemosiderin, Schwietzer<sup>11</sup> suggested that the iron core of this protein has the  $\gamma$ - $\text{FeOOH}$  structure. Wöhler<sup>12</sup> and Fischbach et al.<sup>13</sup> have found, however, that if the ferritin or haemosiderin solid is isolated at room temperature, there is no trace of either  $\alpha$ - or  $\gamma$ - $\text{FeOOH}$  and that the early report of Schwietzer was an artifact of the method of preparation.

Utilizing low-angle X-ray scattering data obtained on iron-containing polymers, Brady et al.<sup>14</sup> have suggested that

**Table I.** Iron Environment in the Fe-Glycine Model Compound as Determined by X-ray Diffraction<sup>a</sup>

type of atom	<i>N</i>	<i>R</i> , Å
oxygen	1	1.906
oxygen	4	2.025
oxygen	1	2.095
carbon	4	2.985
iron	2	3.298
oxygen	4	3.396

<sup>a</sup> *N* is the number of atoms, and *R* is their distance from the iron atom.

the O<sup>2-</sup> and OH<sup>-</sup> ligands are tetrahedrally arranged around the Fe<sup>3+</sup> ions. Gray<sup>15</sup> has questioned this conclusion, citing spectroscopic evidence which suggests an octahedral arrangement of ligands. Gray's position has been supported by spectroscopic results obtained by Holt et al.<sup>16</sup> on model compounds.

Although ferritin can be crystallized, it has not been possible to determine directly the structure of the Fe-containing core by conventional X-ray techniques because the iron cores do not have a definite orientation with respect to the outer shell.<sup>2a</sup> This means that only Debye-Scherrer rings can be obtained for the core, and they are much broadened owing to the small size of the micelle. However, the size of the micelle is not a detriment to analysis of the local iron environment by the extended X-ray absorption fine structure (EXAFS) technique. Also, measurement of the structure in the Fe K-edge can provide information about the chemical state of the iron.

The EXAFS spectrum from a single shell of *N* identical atoms at an average distance *R* from the absorbing atom can be written as<sup>17</sup>

$$\chi(k) = \frac{N}{R^2} B(k) e^{-2(k^2\sigma^2 + R/\lambda)} \sin(2kR + \delta(k)) \quad (1)$$

where *B*(*k*) is proportional to the backscattering amplitude, which depends on the type of scattering atom,  $\delta(k)$  is the phase,  $\lambda$  is the electron mean free path, and  $\sigma^2$  is the mean square deviation from the average distance *R*.  $\sigma^2$  is a measure of the disorder in the bond lengths and can be due either to thermal vibrations or an inherent small structural disorder. The total EXAFS spectrum is given by a sum of contributions from each individual shell of atoms.

In order to accurately account for *B*(*k*),  $\delta(k)$ , and  $\lambda$ , it is necessary to make the same absorption measurements on well-characterized standard compounds for which the iron has a similar chemical environment. In this paper we will concentrate on a comparison between ferritin and the Fe-glycine compound tri- $\mu_3$ -triaquo-hexakis(glycine)triiiron(III) perchlorate. Its structure at room temperature has been determined by X-ray diffraction studies,<sup>18</sup> and it was found that the iron is in trimeric units with six first neighbors oxygens. The Fe environment in this compound is summarized in Table I. This material should be a good standard compound since the optical absorption and magnetic properties have been shown to resemble those of ferritin.<sup>16,19</sup>

Another interesting model for ferritin is the polymer of Spiro and Saltman<sup>21</sup> which has a composition of Fe<sub>4</sub>O<sub>3</sub>(OH)<sub>4</sub>(NO<sub>3</sub>)<sub>3</sub>·1.5H<sub>2</sub>O. This Spiro-Saltman ball has a molecular weight of about 150 000 and is about 70 Å in diameter, very similar in size to the ferritin micelle. The structure of this polymer is not known, but low-angle X-ray scattering experiments<sup>14</sup> suggest fourfold coordination of the irons while the electronic absorption spectra indicate an octahedral coordination.<sup>15</sup> We have also made EXAFS measurements on this polymer, which we found to be composed of two differing fractions.

## II. Experimental Section

The ferritin sample was commercially available<sup>20</sup> horse spleen ferritin in water solution at a concentration of 25 mg/mL. The sample was electrophoretically homogeneous and displayed an optical absorption maximum at about 920 nm as reported earlier.<sup>15</sup> The preparation of the Fe-glycine standard compound has been described elsewhere.<sup>21</sup>

The Spiro-Saltman polymer was prepared as described by Spiro et al.<sup>22</sup> When this was done, the previously reported soluble fraction, eluted with the void volume, was obtained. After considerable further elution a second fraction was obtained which could not be redissolved after drying. We will call these fractions A and B, respectively. Since previous experiments<sup>14,15</sup> did not distinguish between these two forms of this polymer, we report here the results for both. These measurements were made on the dried powder forms.

Another standard compound, which was measured at both room temperature and 80 K, was the mineral goethite which has the  $\alpha$ -FeOOH structure. This was meant to be used as a standard for both the first and second shells, but the powder samples that we used turned out to have a preferred orientation of the crystalline grains. Since this material is anisotropic this made the second-shell results unreliable. However, the first shell has sufficient symmetry so that the first-shell results could be used as a standard for Fe-O EXAFS. For an additional standard for Fe-Fe scattering an Fe foil was also measured.

The X-ray absorption measurements were performed at the Stanford Synchrotron Radiation Laboratory (SSRL). Most of the measurements were made on the focused X-ray line, which has a resolution of about 10 eV. Some higher resolution studies were made on line 11 with a resolution of 2 eV. All of the spectra were taken in absorption. Measurements on the ferritin solution were made at 80, 120, 160, 210, and 293 K. For the low-temperature measurements, the solution was frozen, and it will be shown in our measurements that the iron environment in ferritin distorts somewhat. This indicates that a structural change is occurring at low temperature. Several measurements were made on each sample at each temperature. No differences were found between repetitive runs which indicates that degradation by the X-ray beam was negligible.

The Fe-glycine standard was measured in powder form at room temperature and 80 K, but the 80 K data did not agree with the room temperature results. This again indicates that some type of structural change is occurring at low temperatures. The two forms of the Spiro-Saltman ball were measured at room temperature and 80 K and a normal temperature dependence was found.

Some examples of the room temperature data are shown in Figure 1. Both complete scans and expanded plots of the near edge structure are shown in (a). In (b) the EXAFS is shown after the background has been removed, and the energy scale has been converted to the photoelectron wave vector *k*. For all spectra, *k* = 0 was defined as the position of the small "pip" just before the edge which is indicated by the arrow in Figure 1a. For the low-resolution focused line results this pip is not resolved, and the *k* = 0 point is found by comparing the edges with those taken at high resolution to determine where the pip would appear if it were resolved.

## III. Analysis and Discussion

**A. Ferritin.** The analysis of EXAFS spectra, as in Figure 1b, has been well described<sup>17</sup> previously, and only the important parts of the analysis will be discussed here. A Fourier transform of the EXAFS spectra yields a radial distribution function with peaks corresponding to the locations of the various shells of atoms surrounding the absorbing iron atom. Because of phase shift effects ( $\delta(k)$  in eq 1), the peaks in the transforms are shifted from the actual interatomic distances. Some transforms of the data in Figure 1 are shown in Figure 2.

For both the ferritin and the Fe-glycine data, two types of transforms are shown in Figure 2. The EXAFS  $\chi(k)$  has been multiplied by both *k* and *k*<sup>3</sup> before transforming, and for both the *k*<sup>3</sup> transforms (solid lines), the second-shell peak is enhanced somewhat compared to the first-shell peak. For the Fe-glycine data in Figure 2a, the considerable interference in the second shell between the contributions from the low *Z* atoms and the irons present in the *k* transform (which tends to cancel the peak) is largely absent in the *k*<sup>3</sup> transform. This

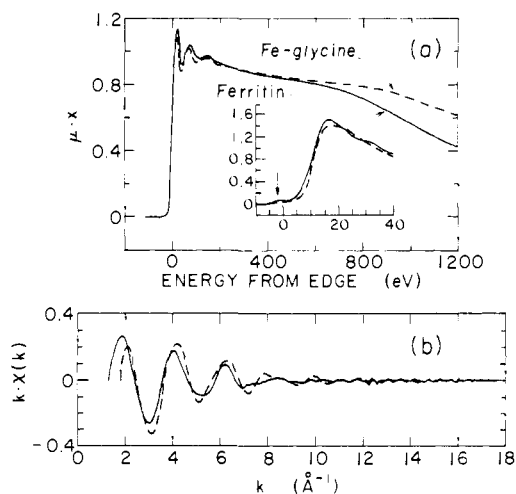


**Figure 1.** EXAFS data for ferritin and the Fe-glycine standard taken at room temperature. (a) Complete scans with the background removed and the edge steps normalized to one. The insert gives a high-resolution view of the near-edge structure. The long scans were taken on the focused EXAFS line and the edge structure was obtained at higher resolution on EXAFS line II. (b)  $\chi(k) \cdot k$  vs.  $k$  for the scans in (a).

can be explained by the differing  $k$  dependence of the back-scattering amplitude  $B(k)$  for different types of atoms. Weighting the data by  $k^3$  enhances the contribution to the transform of the heavier atoms. Since the ferritin data in Figure 2b show a small enhancement of the second shell, it also seems to have iron neighbors in the second shell. In comparing these  $k$  and  $k^3$  transforms, it should be remembered that the second shell likely has a larger thermal Debye-Waller factor. Thus, one would expect a low  $Z$  second-shell peak to be reduced relative to the first shell in a  $k^3$  transform. Furthermore, the much reduced interference (the second peak is better resolved) in the Fe-glycine  $k^3$  weighted transform indicates the second shell peak is dominated by the iron contribution. Additional evidence for identifying the second shell in ferritin as iron is given later in this section.

Therefore, from transforms such as those in Figure 2, we can conclude that the iron environment in ferritin is similar to that of the Fe-glycine standard, with light atom first shell neighbors at  $1.95 \pm 0.02 \text{ \AA}$  and iron neighbors at  $3.29 \pm 0.05 \text{ \AA}$ . These values were obtained by using the standards to correct for the peak shifts due to the phase shift  $\delta(k)$ . From the stoichiometry of the iron core in ferritin, the nearest neighbors must be oxygens.

The errors in the above values have two major contributions. The first includes all statistical and systematic errors. They are due to noise and systematic errors introduced by the analysis procedure. These contributions are easily estimated by comparing the results of analyzing repeated scans using varying analyzing parameters. The second source of possible error is the variations of the peak shift caused by possible differences in the phase shift  $\delta(k)$  under varying chemical environment. These peak shifts are transferable for materials with similar Fe environments if the two sets of data are analyzed identically. We checked for possible variation by comparing two standards, Fe-glycine and  $\alpha$ -FeOOH, whose chemical variation is similar to that between themselves and ferritin. For the Fe-glycine compound this peak shift is  $0.46 \pm 0.01 \text{ \AA}$  for the first shell and the  $k^3$  transform shown in Figure 2, while for  $\alpha$ -FeOOH it is  $0.47 \pm 0.01 \text{ \AA}$ . For the ferritin first-shell distance the average of these results was used. The second-shell peak shift was found to be  $0.45 \pm 0.02 \text{ \AA}$  using the Fe-glycine standard.

All of the ferritin results are given in Table II. In spite of possible distortions, the first-shell distance seems to be tem-

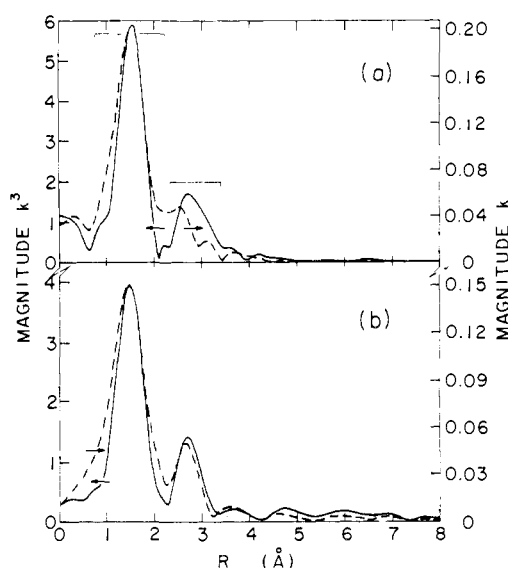


**Figure 2.** Fourier transforms of  $k \cdot \chi(k)$  and  $k^3 \cdot \chi(k)$  for (a) Fe-glycine, (b) ferritin. The dashed lines are the  $k$  weighted transforms and the solid lines the  $k^3$  weighted transforms. These transforms were taken over a  $k$ -space range of  $2.5$ – $10.5 \text{ \AA}^{-1}$  with a Hanning cutoff applied to the data from  $2.5$  to  $4 \text{ \AA}^{-1}$  and  $9$ – $10.5 \text{ \AA}^{-1}$ . The horizontal bars show the  $r$ -space ranges used for isolating and comparing the first two peaks in ferritin with those from the standard.

**Table II.** EXAFS Results for Ferritin as a Function of Temperature<sup>a</sup>

$T$ , K	$N$	$R$ , $\text{\AA}$	$\sigma^2 - \sigma^2$ (Fe-Gly), $\text{\AA}^2$
1st Shell Oxygen			
293	$6.4 \pm 0.6$	$1.95 \pm 0.02$	$0.0057 \pm 0.0005$
210	$7.4 \pm 2.0$	$1.97 \pm 0.03$	$0.0150 \pm 0.003$
160	$7.4 \pm 1.0$	$1.92 \pm 0.02$	$0.0112 \pm 0.0005$
115	$7.1 \pm 0.8$	$1.95 \pm 0.02$	$0.0107 \pm 0.0005$
80	$5.8 \pm 1.3$	$1.94 \pm 0.03$	$0.006 \pm 0.003$
2nd Shell Iron			
293	$7 \pm 1$	$3.29 \pm 0.05$	$0.015 \pm 0.003$
210	$10 \pm 3$	$3.35 \pm 0.1$	$0.020 \pm 0.008$
160	$11 \pm 3$	$3.36 \pm 0.1$	$0.015 \pm 0.005$
115	$7 \pm 1$	$3.38 \pm 0.1$	$0.011 \pm 0.003$
80	$10 \pm 3$	$3.35 \pm 0.1$	$0.012 \pm 0.005$

<sup>a</sup> For both the first-shell and the second-shell irons, the coordination number  $N$ , average bond distance  $R$ , and the mean square displacement of  $R$  about the average value are listed. The  $\sigma^2$  values are increased relative to the Fe-glycine model compound.

perature independent. For the Fe-Fe distance, the low-temperature values are consistently higher than the room temperature distance. This is likely due to interference with a third peak near  $3.8 \text{ \AA}$  which becomes visible as a shoulder to the second shell at low temperatures.

Further comparison of the two sets of data can also be done to determine the number of atoms and  $\sigma^2$  for each shell. Again, this procedure is described in detail in ref 15, and involves transforming the individual peaks of the radial distribution function back to  $k$  space in order to determine envelope functions for the oscillations from each shell separately. From eq 1 we see that the magnitudes of these envelope functions are determined by the number of neighbors  $N$ , and the  $k$  dependence is determined by  $B(k)$  and the Debye-Waller factor. Since the chemical environments of the iron atoms are similar for the two materials, the function  $B(k)$  should be the same, and any differences in the envelope functions are due to differences in  $N$  and  $\sigma^2$ .

We have compared ferritin with the Fe-glycine standard

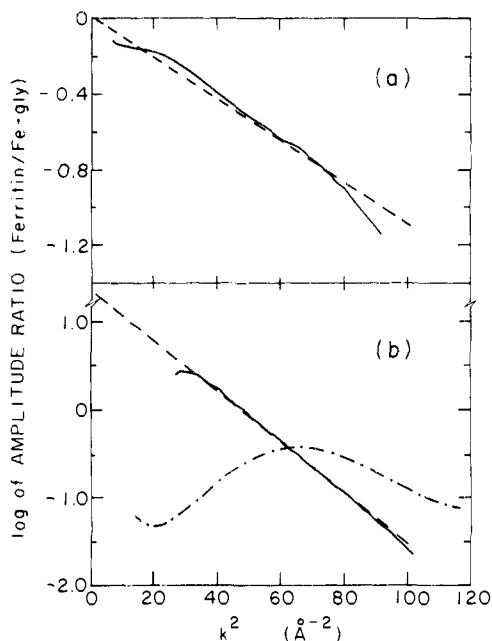


**Figure 3.** Examples of plots used to compare the coordination and disorder of the first two shells in ferritin with the corresponding shells in the Fe-glycine model. Plotted are the logarithms of the ratio of envelope functions vs.  $k^2$  for the first shells of each (a); the second shells of each [(a) solid curve]; and [(b) dot-dashed curve] the second shell of ferritin over the first shell of Fe-glycine.

using the  $r$ -space windows shown in Figure 2 to isolate the two shells. The logarithms of the ratio of the resulting envelope functions were then plotted vs.  $k^2$  as shown in Figure 3. If the backscattering amplitude  $B(k)$  is the same for the two materials, then these plots should yield straight lines with an intercept determined by the ratio of coordination numbers and distances, and a slope due to differences in  $\sigma^2$ . The factor  $B(k)$  depends on only the type of backscattering atom for similar chemical environments around the irons, as is the case here.

In Figure 3 good straight lines are obtained, except at high  $k$ , where noise begins to dominate the data. These straight lines confirm our previous conclusions that the first shell in ferritin is composed of oxygens and the second shell of irons. As a further check a similar plot was made comparing the first shell of the standard which contains oxygen with the second shell of ferritin, and is shown as the dot-dashed curve in Figure 3. Clearly the functions  $B(k)$  are different because a straight line is not found, confirming that the second shell of ferritin is not predominantly oxygen. For the first-shell ratio plot the intercept is near zero indicating that the coordination number in ferritin is nearly the same as for the Fe-glycine standard. For the second shell, the coordination number in ferritin is considerably higher than the standard, corresponding to about seven iron atoms. The slopes of these lines indicate that both coordination shells in ferritin are more disordered than the standard. Table II summarizes these results along with similar ones obtained from the low-temperature data. Just as for the bond length results, the statistical and systematic errors were obtained by comparing results from different scans and by using different  $r$ -space ranges. The transferability of the function  $B(k)$  was checked by comparing with both the Fe-glycine and  $\alpha$ -FeOOH standards.

It is in the first-shell  $\sigma^2$  results that the evidence for distortion at low temperatures is clearest. At low temperature, the disorder increases considerably when it would be expected to decrease as thermal vibrations are frozen out. Because of this result, only the room temperature values should be considered representative of the iron environment in ferritin in its biologically active form. Our measurements show that because

of this structural change, care must be exercised in analyzing data taken on ferritin at low temperatures. This point is particularly important for such measurements as Mössbauer and magnetic susceptibility measurements which are often done as a function of temperature. Similarly, the 80 K Fe-glycine data were analyzed and an increase in  $\sigma^2$  was also found for the first shell. At 80 K,  $\sigma^2$  increases by  $0.0020 \pm 0.0005$  and the coordination number decreases by about one atom, indicating a phase transition occurring at low temperature for this standard, also.

From Table I, we see that the second shell of the Fe-glycine standard has a considerable contribution from oxygen and carbon neighbors. In spite of the  $k^3$  weighting, these could add uncertainty to the Fe-Fe coordination, and so additional checks were made. It was found that for the higher resolution line II results, there was a significant contribution to the second-shell envelopes for  $k \lesssim 5 \text{ \AA}^{-1}$  from these low  $Z$  atoms. However, this was not a problem for the low resolution focused line results, presumably because the sharp structure at low energies due to the low  $Z$  atoms was not fully resolved. When only the data for  $k \gtrsim 5 \text{ \AA}^{-1}$  from line II was used, the same results as for the focused line were obtained, demonstrating that any interference from the second-shell oxygens and carbons in the Fe-glycine standard is small. It should also be noted that the interference found for the second-shell Fe-glycine envelopes was not seen in the high-resolution ferritin data taken at room temperature. This indicates that the second shell of ferritin contains predominantly iron. Since there is a third shell which shows up in the low-temperature data, and seems to show low  $Z$  behavior, it appears that in ferritin the bulk of the second neighbor oxygens are located at a larger distance than the iron shell. However, this third shell could also be due to the distortion caused by freezing the solution. More data are needed to clarify this result.

Another check which was made on the second-shell results was to compare them with data from iron foil. In this case we can be certain that the neighbors are only iron atoms, but because of the different chemical environment these comparisons are not as accurate as using the glycine standard compound. However, the results of the comparisons were in good agreement with those obtained using the Fe-glycine standard, and we can be confident that our results on the second shell are correct.

We now turn our attention to the near edge structure shown in Figure 1. The edges are similar; in particular the magnitudes of the first large peaks are about the same, although the finer details show differences. This reflects the fact that the iron environment in ferritin is similar to but not identical with that of the standard. Of particular interest is the small "pip" just before the edge indicated by the arrow. This is due to transitions to iron 3d states. These transitions are forbidden if the iron site has inversion symmetry as would be the case for octahedral coordination. It is present in the standard, since the first shell is distorted from a true octahedron. In ferritin the pip is somewhat larger. This is consistent with a greater disorder of the first-shell oxygens, which was also found in the EXAFS analysis. For comparison, the pip in rubredoxin,<sup>23</sup> which has its iron tetrahedrally coordinated with sulfurs, has about twice the intensity of that found in ferritin. Also, we have measured the pip in  $\text{Fe}_3\text{O}_4$  and found it to be about 1.5 times stronger than that in ferritin. This material has the spinel structure with  $1/3$  of the irons tetrahedrally coordinated and  $2/3$  octahedrally coordinated. An estimate of the size of the pip for tetrahedral environment alone can be obtained by multiplying by 3 since the octahedral sites will give little contribution. Thus tetrahedral sites would give a pip about 4.5 times the size of that found in ferritin.

**B. Spiro-Saltman Ball.** The data from the two forms of the iron polymer of Spiro and Saltman were analyzed in the same

**Table III.** EXAFS Results for the Two Forms of the Spiro-Saltman Ball<sup>a</sup>

<i>T</i> , K	<i>N</i>	<i>R</i> , Å	$\sigma^2 - \sigma^2$ (Fe-Gly), Å <sup>2</sup>
Form A			
1st shell oxygen			
293	3.6 ± 0.4	2.00 ± 0.02	0.0025 ± 0.0005
80	3.7 ± 0.4	1.99 ± 0.02	0.0010 ± 0.0004
2nd shell iron			
293	4.1 ± 0.6	3.34 ± 0.08	0.0143 ± 0.0030
80	3.9 ± 0.7	3.44 ± 0.06	0.0104 ± 0.0025
Form B			
1st shell oxygen			
293	5.4 ± 0.6	1.97 ± 0.02	0.0045 ± 0.0008
80	5.3 ± 0.6	1.98 ± 0.02	0.0030 ± 0.0006
2nd shell iron			
293	6.6 ± 1.1	3.33 ± 0.06	0.0147 ± 0.0030
80	5.2 ± 0.9	3.36 ± 0.07	0.0093 ± 0.0023

<sup>a</sup> *N* is the coordination, *R* is the average bond distance, and  $\sigma^2$  is the mean square displacement of *R* relative to the Fe-glycine model compound.

manner as the ferritin data. Again the Fe-glycine compound was used as a standard to determine *R*, *N*, and  $\sigma^2$ . As for ferritin, the first shell was found to be oxygen and the second shell was found to contain iron. Our results are summarized in Table III. Although the distances are similar to ferritin, the coordinations for the two forms are different. Also, in contrast to ferritin, the behavior of  $\sigma^2$  with temperature is normal. From these results we can conclude that form A of the Spiro-Saltman ball is not a good model for ferritin while form B is possibly similar.

Our results for form A are, moreover, in good agreement with earlier X-ray scattering results.<sup>14</sup> On the basis of these earlier results a model was suggested which consisted of planar structure with the irons tetrahedrally coordinated, although optical absorption measurements<sup>14,15</sup> were not in agreement with tetrahedral coordination. Even though they find four neighbors, our measurements for form A are not consistent with tetrahedral coordination since the near edge 3d pip was found to be slightly smaller than Fe<sub>3</sub>O<sub>4</sub>, which has only 1/3 of its irons tetrahedrally coordinated. Therefore, the average iron site in form A must be considerably more centrosymmetric than a tetrahedral coordination, although the coordination is about four, indicating that the four Fe neighbors are more planar than tetrahedral. The results for form B are, however, consistent with a distorted octahedral coordination of the irons. The existence of these two different forms of this polymer may explain the apparent conflict of the earlier measurements. Work on these polymers is continuing and a more detailed description will be published later.

#### IV. Structure of the Ferritin Micelle

By combining the EXAFS results with the known stoichiometry and density of the ferritin micelle, its average structure can be deduced. From the value of  $\sigma^2$  for the Fe-Fe distance we find that the average deviation in Fe-Fe distances is only slightly greater than 0.1 Å. The average volume per Fe atom is then rather well defined, and the volume does not vary much around each Fe atom even if the Fe has different inequivalent sites.

The EXAFS results for the Fe-Fe coordination allow six-, seven-, or eightfold coordination. For a three-dimensional structure with sixfold Fe-Fe coordination, the arrangement of the Fe atoms must be based on a simple cubic lattice in order for all the Fe-Fe distances to be nearly the same. This is shown in Figure 4a. Since each Fe atom has associated with it an oxygen atom and a hydroxy group, the density of this structure is easily calculated. Using the EXAFS Fe-Fe distance of 3.29

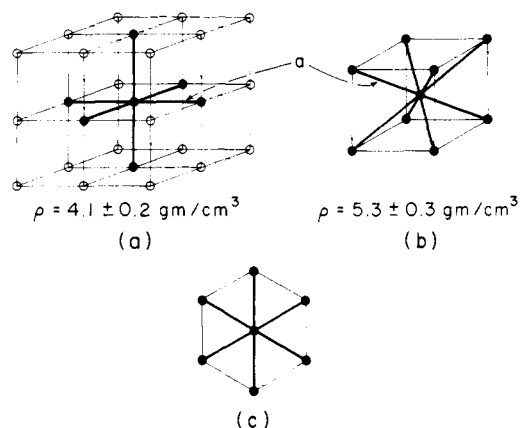


**Figure 4.** Types of average long-range order allowed by the EXAFS results. Only the iron positions are shown. The densities are calculated using  $a = 3.29 \pm 0.05$  Å.

$\pm 0.05$  Å the density of this type of structure is  $4.10 \pm 0.2$  g/cm<sup>3</sup>. The  $\sigma^2$  results mean that this cubic structure can be distorted slightly, for example, giving orthorhombic symmetry. However, since the average Fe-Fe distance must remain the same, calculations show the density to be only slightly affected by these distortions.

The density of the ferritin micelle has been determined in two independent ways. Granick and Hahn<sup>3</sup> in their work on the chemical composition of the micelle gave a value of 3.50 g/cm<sup>3</sup> if the micelle composition is (FeOOH)<sub>8</sub>(FeO·OPO<sub>3</sub>H<sub>2</sub>) and a value of 3.83 g/cm<sup>3</sup> if the composition is assumed to be pure FeOOH. Since then, many authors<sup>26</sup> have confirmed the existence of phosphorus in the micelle, and the lower density should be the best. Strong confirmation of this value is provided by the low-angle X-ray scattering work of Fischback and Anderegg.<sup>24</sup> They independently determined the average size of the micelle and the amount of Fe which it contains. From these numbers the density of the micelle can be calculated if its composition is known. Again assuming the composition of Granick and Hahn<sup>3</sup> gives a density of 3.4–3.5 g/cm<sup>3</sup>. In this case assuming pure FeOOH would result in a lower density in contrast to the method of Granick and Hahn which would give a higher density. Thus, the two independent determinations give a density of the micelle close to 3.5 g/cm<sup>3</sup>, and a three-dimensional structure with sixfold Fe-Fe coordination is not allowed.

Similarly, a three-dimensional structure with eightfold Fe-Fe coordination must be based on a body-centered cubic type structure as shown in Figure 4b. In this case, the density is even higher at  $5.3 \pm 0.3$  g/cm<sup>3</sup>. This density can be lowered somewhat by the distortions allowed by our  $\sigma^2$  result, but it is always greater than the corresponding sixfold coordinated structure. For the case of strict sevenfold coordination there are no lattice arrangements possible in three dimensions. It is possible to achieve an average sevenfold coordination by a combination of sixfold and eightfold coordination, but from the above arguments the density of this type of structure would also be too high. Thus, the EXAFS results combined with density measurements rule out all three-dimensional non-layered structures.

In order to achieve the measured density, we have to consider two-dimensional layered structures. In this case the separation between the layers can be varied to obtain the proper density. In two dimensions the maximum rotational symmetry allowed is sixfold. If inequivalent Fe sites exist, they are expected not to have large differences according to our EXAFS results. Besides the fact that the Fe-Fe distance is reasonably uniform, the Fe-O distance is also reasonably uniform, with an average deviation of about 0.1 Å from the bond length of 1.95 Å. The

**Table IV.** Comparison of the  $\alpha$ - and  $\gamma$ -FeOOH Structures with Ferritin, and the Two Forms of the Polymer of Spiro and Saltman<sup>a</sup>

	1st shell			2nd shell irons			$\rho$ , g/cm <sup>3</sup>
	$N$	$R$ , Å	$\sigma_s^2$ , Å <sup>2</sup>	$N$	$R$ , Å	$\sigma_s^2$ , Å <sup>2</sup>	
$\alpha$ -FeOOH	6	2.02	0.0049	8	3.32	0.030	4.20
$\gamma$ -FeOOH	6	2.01	0.015	6	3.05	0.0001	4.02
$\alpha$ -FeOOH (110)	6	2.02	0.0049	6	3.27	0.029	
ferritin	$6.4 \pm 0.6$	$1.95 \pm 0.02$	$0.0089 \pm 0.0005$	$7 \pm 1$	$3.29 \pm 0.05$	$0.015 \pm 0.003$	3.4-3.5
Spiro-Saltman							
ball fraction "A"	$3.6 \pm 0.4$	$2.00 \pm 0.02$	$0.0057 \pm 0.0005$	$4.1 \pm 0.6$	$3.34 \pm 0.08$	$0.0143 \pm 0.003$	2.9-3.0
fraction "B"	$5.4 \pm 0.6$	$1.97 \pm 0.02$	$0.0045 \pm 0.0008$	$6.6 \pm 1.1$	$3.33 \pm 0.06$	$0.0147 \pm 0.003$	

<sup>a</sup>  $N$  is the coordination,  $R$  is the average bond length,  $\sigma_s^2$  is the mean square structural disorder associated with  $R$ , and  $\rho$  is the density. Also included for comparison are the values for a single (110) layer in the  $\alpha$ -FeOOH structure. The  $\sigma_s^2$  for ferritin and the Spiro-Saltman ball were determined using the known structural disorder of the Fe-glycine model and assuming that the thermal contribution to  $\sigma^2$  is the same for the three materials.

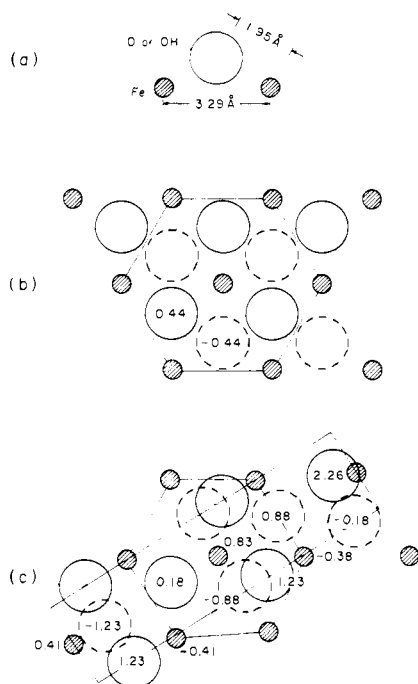


**Figure 5.** (a) Average structural unit determined by the EXAFS measurements. (b) Idealized model structure constructed using the unit in (a) and the long-range symmetry of Figure 4c. (c) Top view of the (110) plane in  $\alpha$ -FeOOH. The numbers are the vertical positions of the atoms in ångströms.

only reasonable way to satisfy our EXAFS results is for each Fe site to have approximate sixfold symmetry, as in Figure 4c, since in two dimensions the maximum rotational symmetry allowed is sixfold, the same as the average symmetry.

Since we have determined the average symmetry of the iron core we can now construct its average structure. To do this we consider the EXAFS information obtained for the first shell. Including these results for the Fe-O distance requires that the building block of the ferritin structure must be as shown in Figure 5a. Using these units in the two-dimensional structure shown in Figure 4c gives the results shown in Figure 5b. It should be emphasized that this structure is the only one which is consistent with all the experimental data. It is a layered structure with hexagonal symmetry and a flattened octahedral arrangement of oxygens about each iron. For the proper stoichiometry, half of the oxygen ligands would be OH. For the proper density these layers must be on the average  $\geq 4.6$  Å apart, depending on the amount of water or other material between the planes. Thus, the planes are likely only weakly bound together.<sup>25</sup>

The arrangement in Figure 5b is an average one, and not meant to represent the actual atomic positions. From the  $\sigma^2$

results we know that there is significant disorder within this average with the average displacement of the Fe-O and Fe-Fe distances being approximately 0.1 Å. This disorder would almost certainly cause the oxygen ligands to assume a more octahedral arrangement, since in this average structure some of the O-O distances are anomalously short at approximately 2.2 Å.

In Table IV it is shown that the ferritin core is different from both the  $\alpha$ - and  $\gamma$ -FeOOH structures.<sup>26,27</sup> However, there are similarities between these structures and our result for ferritin. Both have some layered character to their structure. In particular the (110) plane in the  $\alpha$ -FeOOH structure is very reminiscent of our ferritin result and is shown in Figure 5c. This also gives an example of the types of distortions which must be present in the ferritin lattice. In addition, the similarity of this structure with that of ferritin provides an explanation of the observations of Wöhler.<sup>12</sup> He found that if ferritin is dried at 100 °C over P<sub>2</sub>O<sub>5</sub>, its X-ray diffraction pattern converted to a mixture of the  $\alpha$ - and  $\gamma$ -FeOOH patterns.

To complete the structure of ferritin the P must be accounted for. In the two-dimensional structure of ferritin the P plays a natural role of terminating the sheet into a form of a strip. From the stoichiometry, 2P would be needed to terminate 18Fe along the width of the strip. One way to accomplish this which is consistent with the stoichiometry is illustrated in Figure 6a. In this case all the iron sites are equivalent and the width of the strip is approximately 60 Å. This is consistent with the micellar core diameter of about 70 Å.

## V. Conclusions

The EXAFS measurements have provided a considerable amount of direct structural information about the iron core in ferritin, which is summarized in Table IV. These results have allowed us to determine the average structure of the micelle. Our value for the first-shell coordination number of  $6.4 \pm 0.6$ , and an examination of the strength of the 3d pip, confirms the previously suggested<sup>15,16</sup> octahedral arrangement of near-neighbor ligands. The measurements also show that on the average the ligands are distorted somewhat from a regular octahedron. This may explain some of the difficulties in previous determinations of site symmetry. These measurements also provide the first structural information about the second shell, which turned out to contain  $7 \pm 1$  irons at a distance of  $3.29 \pm 0.05$  Å according to our EXAFS results alone.

It is the second-shell results which are crucial in our determination of the structure of the micelle. When combined with the known stoichiometry and density of the micelle these results ruled out all three-dimensional structures. It was found that only a two-dimensional layered type structure would account for all the experimental results. In this structure, which is shown in Figure 5b, a plane of iron atoms is sandwiched between two layers of approximately close-packed oxygens. These three atom thick layers are then only weakly bound together

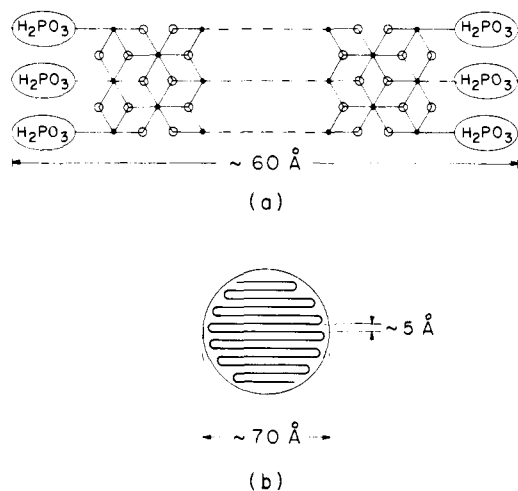


**Figure 6.** (a) One way of using the phosphorus atoms to terminate the two-dimensional sheets of Figure 5b into a strip. The solid circles are iron and the larger open circles are O or OH. From the stoichiometry there are 9 Fe per P, giving a width of  $\sim 60$  Å. The length of the strip depends on the amount of iron in the micelle. (b) Schematic drawing of the folding of the strip into a 70-Å diameter micelle.

to form the three-dimensional micelle. The phosphorus atoms are accounted for by assuming that they terminate the sheet into a strip whose width naturally accounts for the size of the micelle of about 70 Å as illustrated in Figure 6a.

This result is also attractive from the viewpoint of iron mobilization. It is known that as the iron core is depleted of iron it assumes a flattened shape with one dimension shrinking while the others remain nearly the same, spanning the inner chamber of the protein.<sup>24</sup> This seems difficult for a three-dimensional lattice since it requires the removal of iron from the parts of the core which has lost contact with the outer protein sheath. In a layered structure, however, the ends of the strip can remain in contact with mobilization sites in the sheath, with the strip changing length as iron is mobilized. In fact, it is our picture that the iron core is one single strip which is folded back and forth upon itself, as in a pleat. This is illustrated in Figure 6b. The amounts of disorder found in the lattice would certainly allow this possibility.

Another important result from these measurements is the distortion in the iron environment which was observed as the solution is frozen. The accessibility of the irons to the distortions of the water on freezing is easily understood in the two-dimensional structures. This distortion does not seem to have been noted previously, and has an important bearing on the interpretation of measurements made at low temperatures, such as Mössbauer and magnetic susceptibility measurements. It should be recognized that such measurements may not be representative of the biologically active form of the protein.

Finally, our measurements have shown that two forms of the polymer of Spiro and Saltman exist and only one is possibly similar to ferritin. The results, which are summarized in Table III, show fourfold oxygen coordination for form A, in good agreement with previous X-ray scattering results, while form B has a sixfold oxygen coordination.

**Acknowledgments.** We are pleased to acknowledge our thanks to the staff of SSRL for their cooperation and help in making these measurements. We are also thankful to G. Bunker and E. Sevillano for their help with the data analysis and to Dr. D. E. Sayers for his helpful conversations and aid in making the measurements. This work was supported in part by the National Science Foundation in cooperation with the U.S. Department of Energy under Research Grants PCM 76-21849 and DMR 77-22955.

## References and Notes

- (1) (a) University of Washington; (b) University of Wyoming.
- (2) (a) P. M. Harrison and T. G. Hoy, "Inorganic Biochemistry", Vol. 1, G. L. Eichhorn, Ed., American Elsevier, New York, N.Y., 1973, p 253; (b) R. R. Crichton, *Struct. Bonding (Berlin)*, **17**, 67 (1973).
- (3) S. Granick and P. F. Hahn, *J. Biol. Chem.*, **155**, 661 (1944).
- (4) J. L. Farrant, *Biochem. Biophys. Acta.* **13**, 569 (1954).
- (5) P. M. Harrison, *J. Mol. Biol.* **6**, 404 (1963).
- (6) H. J. Belig, O. Kratky, G. Rohms, and H. Wawra, *Biochem. Biophys. Acta.* **112**, 110 (1966).
- (7) A. Blaise, J. Chappert, and J. Giradet, *C. R. Acad. Sci.*, **261**, 2310 (1965).
- (8) J. F. Boas and B. Window, *Aust. J. Phys.*, **19**, 573 (1966).
- (9) K. S. Murray, *Coord. Chem. Rev.*, **12**, 1 (1974).
- (10) J. A. Thich, C. C. Ou, D. Powers, B. Vasiliou, D. Mastropalo, J. A. Potenya, and H. J. Schugar, *J. Am. Chem. Soc.*, **98**, 1425 (1976).
- (11) C. H. Schwietzer, *Acta Haematol.*, **10**, 174 (1953).
- (12) F. Wöhler, *Acta Haematol.*, **23**, 342 (1960).
- (13) F. A. Fischbach, D. W. Gregory, P. M. Harrison, T. G. Hoy, and J. M. Williams, *J. Ultrastruct. Res.*, **37**, 495 (1971).
- (14) G. W. Brady, C. R. Kurkjian, E. F. X. Lyden, M. B. Robin, P. Saltman, T. Spiro, and A. Terzis, *Biochemistry*, **7**, 2185 (1968).
- (15) H. B. Gray, *Adv. Chem. Ser.*, **No. 100**, 365 (1971).
- (16) E. M. Holt, S. L. Holt, W. F. Tucker, R. O. Asplund, and K. J. Watson, *J. Am. Chem. Soc.*, **96**, 2621 (1974).
- (17) E. A. Stern, D. E. Sayers, and F. W. Lytle, *Phys. Rev. B.* **11**, 4836 (1975).
- (18) R. V. Thundathil, E. M. Holt, S. M. Holt, and K. J. Watson, *J. Am. Chem. Soc.*, **99**, 1818 (1977).
- (19) W. F. Tucker, R. O. Asplund, and S. L. Holt, *Arch. Biochem. Biophys.*, **166**, 433 (1975).
- (20) Cd free horse spleen ferritin from Boehringer, Mannheim, West Germany.
- (21) (a) E. M. Holt, S. L. Holt, W. F. Tucker, R. O. Asplund, and K. J. Watson, *J. Am. Chem. Soc.*, **96**, 2621 (1974); (b) W. F. Tucker, R. O. Asplund, and S. L. Holt, *Arch. Biochem. Biophys.*, **166**, 433 (1975).
- (22) T. G. Spiro, S. E. Allerton, R. Bils, J. Renner, P. Saltman, and A. Terzis, *J. Am. Chem. Soc.*, **88**, 2721 (1966).
- (23) See Figure 2 in B. Bunker and E. A. Stern, *Biophys. J.*, **19**, 253 (1977).
- (24) F. A. Fischbach and J. W. Anderegg, *J. Mol. Biol.*, **14**, 458 (1965).
- (25) A layered structure for ferritin with octahedral coordination of the oxygen about the iron has already been suggested by K. M. Towe and W. F. Bradley, *J. Colloid Interface Sci.*, **24**, 384 (1967), though the arrangement of the layers and the irons within the layers differs significantly from our model.
- (26) W. Hoppe, *Z. Kristallogr., Kristallgeom., Kristallphys., Kristallchem.*, **103**; 73 (1940).
- (27) R. W. G. Wyckoff, "Crystal Structures", Vol. 1, Interscience, New York, N.Y., 1963, p 293.